Observation of Quasiparticle Pair Production and Quantum Entanglement in Atomic Quantum Gases Quenched to an Attractive Interaction

Cheng-An Chen,[1] Sergei Khlebnikov,[1,2] and Chen-Lung Hung[1,2,*]
[1]Department of Physics and Astronomy, Purdue University, West Lafayette, Indiana 47907, USA
[2]Purdue Quantum Science and Engineering Institute, Purdue University, West Lafayette, Indiana 47907, USA

(Received 23 February 2021; accepted 8 July 2021; published 6 August 2021)

We report observations of quasiparticle pair production by a modulational instability in an atomic superfluid and present a measurement technique that enables direct characterization of quasiparticle quantum entanglement. By quenching the atomic interaction to attractive and then back to weakly repulsive, we produce correlated quasiparticles and monitor their evolution in a superfluid through evaluating the *in situ* density noise power spectrum, which essentially measures a "homodyne" interference between ground-state atoms and quasiparticles of opposite momenta. We observe large amplitude growth in the power spectrum and subsequent coherent oscillations in a wide spatial frequency band within our resolution limit, demonstrating coherent quasiparticle generation and evolution. The spectrum is observed to oscillate below a quantum limit set by the Peres-Horodecki separability criterion of continuous-variable states, thereby confirming quantum entanglement between interaction quench-induced quasiparticles.

DOI: 10.1103/PhysRevLett.127.060404

Coherent pair-production processes are enabling mechanisms for entanglement generation in continuous-variable states [1,2]. In many-body systems, quasiparticle pair production presents an interesting case, as interaction creates entanglement shared among collectively excited interacting particles. Entanglement distribution through quasiparticle propagation is a direct manifestation of transport property in a quantum many-body system [3,4]. Controlling quasiparticle pair production and detecting entanglement evolution thus opens a door to probing quantum many-body dynamics, enabling fundamental studies such as information propagation [5,6], entanglement entropy evolution [7], many-body thermalization [8], as well as Hawking radiation of quasiparticles and thermodynamics of an analog black hole [9–11].

In atomic quantum gases, coherent quasiparticle pair production can be stimulated through an interaction quench, which results in a rapid change of quasiparticle dispersion relation that can project collective excitations, from either existing thermal or quantum populations, into a superposition of correlated quasiparticle pairs [12–14]. This has led to a prior observation of Sakharov oscillations in a quenched atomic superfluid [13,15]. However, direct verification of quasiparticle entanglement has remained an open question.

An intriguing case occurs when the atomic interaction is quenched to an attractive value. In that case, not only a larger change of quasiparticle dispersion is involved, but there is also an unstable band, in which quasiparticle dispersion $\epsilon(k)$ is purely imaginary, $\epsilon^2(k) < 0$, where k is the momentum wave number. As a consequence, the early-time dynamics is governed by a modulational instability (MI), which continuously stimulates production of quasiparticle pairs, and the ground state becomes unstable with respect to an exponential growth of density waves. This growth leads eventually to wave fragmentation and soliton formation [16]. Although these consequences of MI have been observed [17–21], the early-time evolution itself has only been recently studied [21]. Nevertheless, it is precisely the early-time dynamics that promises MI-enhanced pair production and quantum entanglement. We note there is a parallel scheme using a roton instability for enhanced quasiparticle entanglement generation in dipolar quantum gases [22].

In this letter, we demonstrate MI-enhanced coherent quasiparticle pair production in a homogeneous 2D quantum gas quenched to an attractive interaction, and report an *in situ* detection method that enables direct characterization of quasiparticle entanglement beyond an existing method [9,23]. Specifically, we monitor coherent quasiparticle evolution after quenching the interaction back to a positive value (see Fig. 1 for protocol). Through *in situ* imaging, we analyze the dynamics of density observables by a method analogous to the well-established homodyne detection technique in quantum optics [24–26] and confirm nonclassical correlations, that is, quantum entanglement in quasiparticle pairs.

Our analyses are based on the time evolution of *in situ* density noise, which is a manifestation of interference between quasiparticle excitations and the ground-state atoms that serve as a coherent local oscillator [27]. In Fourier space, the density noise operator can be written as

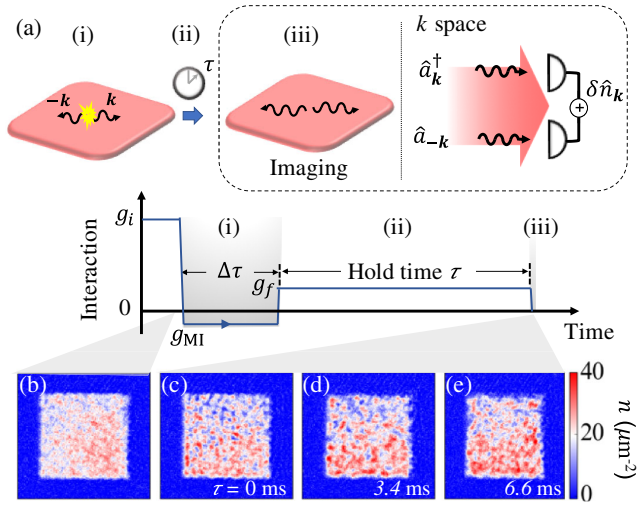

FIG. 1. Experiment scheme for quasiparticle pair production and detection. (a) A homogeneous 2D superfluid (red square) undergoes an interaction quench protocol from (i) $g = g_i > 0$ to $g_{\mathrm{MI}} < 0$ for broadband generation of quasiparticle pairs of opposite momenta (illustrated by black curvy arrows) for a time duration $\Delta\tau$; (ii) a second interaction quench to $g = g_f > 0$ allows quasiparticles to evolve as phonons for a variable hold time τ; (iii) *in situ* density noise in spatial frequency domain $\delta n_{\mathbf{k}}$ is essentially a "homodyne" measurement of excitations in opposite momentum states interfering with ground-state atoms. (b)–(e) Single-shot density images taken prior to (b) or after the interaction quench (c)–(e) and held for the indicated time τ. Image size: $77 \times 77\ \mu\mathrm{m}^2$.

$\delta\hat{n}_{\mathbf{k}} \approx \sqrt{N}(\hat{a}^{\dagger}_{\mathbf{k}} + \hat{a}_{-\mathbf{k}})$, where $N \gg 1$ is the total atom number nearly all accounted for by the ground-state atoms, and $\hat{a}^{(\dagger)}_{\pm\mathbf{k}}$ are the annihilation (creation) operators for $\pm\mathbf{k}$ single-particle momentum eigenstates. They are related to quasiparticle operators $\hat{\alpha}^{\dagger}_{\pm\mathbf{k}}$ by the Bogoliubov transformation. We study the density noise power spectrum $S(\mathbf{k}) = \langle|\delta n_{\mathbf{k}}|^2\rangle/N$, where $\langle\cdots\rangle$ denotes ensemble averaging. Within our resolution limit ($|\mathbf{k}| \lesssim 2.6/\mu\mathrm{m}$), the power spectrum conveniently measures the combined variance of two-mode ($\pm\mathbf{k}$) quasiparticle quadrature operators $\hat{x}_{\mathbf{k}} + \hat{x}_{-\mathbf{k}}$ and $\hat{p}_{\mathbf{k}} - \hat{p}_{-\mathbf{k}}$, where $\hat{x}_{\mathbf{k}} = (\hat{\alpha}^{\dagger}_{\mathbf{k}} + \hat{\alpha}_{\mathbf{k}})/\sqrt{2}$ and $\hat{p}_{\mathbf{k}} = i(\hat{\alpha}^{\dagger}_{\mathbf{k}} - \hat{\alpha}_{\mathbf{k}})/\sqrt{2}$ [28]. Since pair production should be isotropic in our quantum gas samples, in the following we discuss azimuthally averaged spectrum $S(k)$, and use $\pm k$ to denote opposite momenta. In the superfluid ground state absent quasiparticle (phonon) excitations, the Bogoliubov theory predicts $S(k) = C_k$, where $C_k = \epsilon_k/\epsilon(k,g)$ is the ground-state squeezing parameter, ϵ_k the single-particle energy, $\epsilon(k,g) = \sqrt{\epsilon_k^2 + 2(\hbar^2/m)\bar{n}g\epsilon_k}$ the phonon dispersion relation, $\bar{n}$ the mean density, g the interaction at the time of the measurement, m the atomic mass, and $\hbar$ the reduced Planck constant.

In the presence of quasiparticles with nonclassical correlation, the power spectrum would squeeze below the ground-state level, i.e., to $S(k) < C_k$. This intuitive bound can be formally derived following Refs. [29,30], which consider a continuous-variable version of the Peres-Horodecki separability criterion for bipartite entanglement. Adapted to our case [28], the criterion states that the variance of two-mode quadratures must satisfy

$$S(k) = \frac{C_k}{2}[\langle(\hat{x}_k + \hat{x}_{-k})^2\rangle + \langle(\hat{p}_k - \hat{p}_{-k})^2\rangle] \geq C_k \quad (1)$$

in the absence of quasiparticle entanglement. For noninteracting atoms ($g = 0$), $C_k = 1$, and the above inequality represents the limit of atomic shot noise. For phonons in a superfluid ($g > 0$), the separability criterion requires a lower limit ($C_k < 1$).

In the final state of our quench protocol ($g > 0$), coherent quasiparticle pairs interfere, and $S(k)$ should be time dependent. In the special case of noninteracting phonons, that dependence has the form

$$S(k,\tau) = C_k[1 + \bar{N}_k + \Delta N_k \cos\phi_k(\tau)], \quad (2)$$

where $\bar{N}_k = \langle\hat{\alpha}^{\dagger}_k\hat{\alpha}_k\rangle + \langle\hat{\alpha}^{\dagger}_{-k}\hat{\alpha}_{-k}\rangle$ is the mean total phonon number in $\pm k$ modes, $\Delta N_k = 2|\langle\hat{\alpha}_k\hat{\alpha}_{-k}\rangle|$ is the pair-correlation amplitude, and $\phi_k(\tau) = 2\epsilon(k,g)\tau/\hbar + \phi_k(0)$ is the argument of $\langle\hat{\alpha}_k\hat{\alpha}_{-k}\rangle$ that evolves at twice the phonon frequency. In this case, violation of the inequality Eq. (1) is equivalent to having $\Delta N_k > \bar{N}_k$ [31,32]. The presence of maximal two-mode squeezing $S(k)/C_k < 1$ occurs at $\phi_k \approx (2l+1)\pi$, alternating with maximal antisqueezing $S(k)/C_k > 1$ at $\phi_k \approx 2l\pi$ (l is an integer). In practice, oscillations of $S(k)$ are inevitably damped. Nevertheless, $\pm k$ modes are entangled as long as ΔN_k remains larger than $\bar{N}_k$, or more generally $S(k)$ shows squeezing ($< C_k$)—a key signature that we demonstrate in this letter.

To carry out the experiment, we prepare uniform superfluid samples formed by $N \approx 4.9 \times 10^4$ nearly pure Bose-condensed cesium atoms loaded inside a quasi-2D box potential, which compresses all atoms in the harmonic ground state along the imaging (z-) direction [21] with $l_z = 184$ nm being the harmonic oscillator length. A time-of-flight measurement estimates the sample temperature $T \lesssim 8$ nK. Mean atomic surface density $\bar{n} \approx 21/\mu\mathrm{m}^2$ is approximately uniform within a horizontal box the size of $\approx 48 \times 48\ \mu\mathrm{m}^2$. The interaction strength of the quasi-2D gas $g = \sqrt{8\pi}a/l_z$ is controlled by the s-wave scattering length a via a magnetic Feshbach resonance [33], giving an initial interaction strength $g = g_i \approx 0.127$. An uncertainty in g ($\delta g \approx \pm 0.0006$) is primarily contributed by the uncertainty in the magnetic field at the scattering length zero crossing [21].

As illustrated in Fig. 1(a), an MI period is initiated by quenching the atomic interaction (within 0.8 ms) to a negative value $g_{\mathrm{MI}} \approx -0.026$. The quench timescale is short compared with the initial phonon cycle

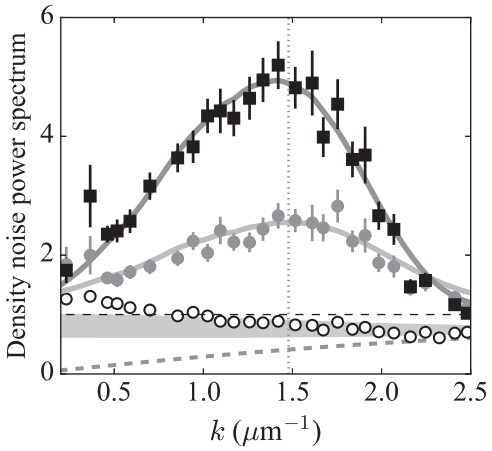

FIG. 2. Growth of density noise during the MI period. Density noise power spectra measured before, $S_0(k)$ (open circles), and right after the MI period, $S(k,0)$, with $\Delta\tau \approx 1$ ms (gray circles) and 2 ms (black squares), respectively. Horizontal dashed line marks the atomic shot-noise level. Gray band represents calculated initial phonon spectrum assuming equilibrium temperature $T = 8 \pm 2$ nK. Dashed curve shows the squeezing parameter C_k at $g = g_i \approx 0.127$. Solid curves are theory fits to data; see text. Vertical dotted line marks the wave number k_c, below (above) which quasiparticles are expected to be unstable (stable) at $g = g_{\mathrm{MI}} \approx -0.026$.

$2\pi\hbar/\epsilon(k, g_i) \gtrsim 2.5$ ms for $k \lesssim 2.6/\mu$m, and the interaction quench is considered quasi-instantaneous. To terminate the MI after additional short hold time $\Delta\tau \approx 1$–2 ms, we quench the atomic interaction back to a small positive value $g_f \approx 0.007$, allowing quasiparticles to evolve as phonons in a stable superfluid for another variable time τ before we perform *in situ* absorption imaging. We have also analyzed quenches without an MI period ($\Delta\tau = 0$). Figures 1(b)–1(e) show sample images measured before and after we initiate the quench protocol. We evaluate $\delta n_{\mathbf{k}}$ for each sample through Fourier analysis [34] and obtain their density noise power spectra. Typically around 50 experiment repetitions are analyzed for each hold time τ. Each power spectrum has been carefully calibrated with respect to the atomic shot noise measured from high temperature normal gases [28,34].

We expect amplified density fluctuations following the MI period due to a sudden change of quasiparticle energy dispersion and pair production [12,13,21]. To quantify the growth of density fluctuations, in Fig. 2 we compare the density noise power spectra measured before and immediately after the MI period, that is, for hold time $\tau = 0$. Before MI, the initial spectrum $S_0(k)$ is mostly below the atomic shot noise due to low temperature $T \lesssim 8$ nK and small initial squeezing parameter $C_k < 1$. Excessive noise in $k \lesssim 0.75/\mu$m may be due to technical heating in the box potential. After the MI time period $\Delta\tau$, we indeed find a significant increase in the density noise, $S(k,0) > 1$. The growth occurs both in the instability band $k \lesssim k_c = 2\sqrt{\bar{n}|g_{\mathrm{MI}}|} \approx 1.5/\mu$m, where the dispersion $\epsilon(k, g_{\mathrm{MI}})$ is purely imaginary, and in the stable regime $k \gtrsim k_c$ as well. Within these short MI periods, we observe the largest growth near $k \approx k_c$, where $\epsilon(k, g_{\mathrm{MI}}) \approx 0$. We comment that for a much longer MI period, density waves in the instability band eventually dominate the noise power spectrum due to continuously stimulated quasiparticle pairs, as observed in [21].

Our measured spectra can be well captured by a model that considers coherent evolution from quasiparticle pair production within the Bogoliubov theory and their damping as well as decoherence due to coupling to single-particle Markovian quantum noise (for details, see Supplemental Material [28]). We refer to the coherent signal in the absence of damping as $S_{\mathrm{coh}}(k) = S_0(k)\{1+[(\epsilon(k, g_i)^2 - \epsilon(k, g_{\mathrm{MI}})^2)/\epsilon(k, g_{\mathrm{MI}})^2]\sin^2[\epsilon(k, g_{\mathrm{MI}})\Delta\tau/\hbar]\}$, which describes the hyperbolic growth of density fluctuations in the instability band ($k \lesssim k_c$) [21] and sinusoidal Sakharov oscillations for stable modes ($k \gtrsim k_c$) [13]. On the other hand, quantum noise causes damping (reduction) of the coherent signal and the appearance of an additive incoherent background $S_{\mathrm{inc}}(k)$. The total power spectrum at the end of the MI period is $S(k,0) = e^{-\Gamma_k\Delta\tau}S_{\mathrm{coh}}(k) + S_{\mathrm{inc}}(k)$, where $S_{\mathrm{inc}}(k) = \frac{1}{2}\{\eta_-[\Gamma_k^2/(\Gamma_k^2 + 4\epsilon(k, g_{\mathrm{MI}})^2/\hbar^2)][1 - e^{-\Gamma_k\Delta\tau}(\cos[2\epsilon(k, g_{\mathrm{MI}})\Delta\tau/\hbar] - [2\epsilon(k, g_{\mathrm{MI}})/\hbar\Gamma_k]\sin[2\epsilon(k, g_{\mathrm{MI}})\Delta\tau/\hbar])] + \eta_+(1 - e^{-\Gamma_k\Delta\tau})\}$, with $\eta_\pm = 1 \pm \epsilon_k^2/\epsilon(k, g_{\mathrm{MI}})^2$. The coherent and incoherent contributions are coupled by a k-dependent damping rate Γ_k. Our theory fits (solid curves in Fig. 2) suggest $\Gamma_k \sim 0.5\epsilon_k/\hbar$ [28], which is of the same order of magnitude as the decay rate extracted from the subsequent time-evolution measurements at $g = g_f$ (Fig. 3).

To demonstrate phase coherence and pair correlation in quasiparticles, we plot the complete time and momentum dependence of the density noise power spectrum $S(k, \tau)$, as shown in Fig. 3(a). Here, oscillatory behavior is clearly visible over the entire spectrum. The oscillations are a manifestation of the interference between coherent quasiparticles of opposite momenta $\pm k$, as suggested by Eq. (2), with the relative phase winding up in time as $\phi_k(\tau) = 2\gamma_{k,f}\tau + \phi_0$, where $\gamma_{k,f} = \epsilon(k, g_f)/\hbar$ is the expected Bogoliubov phonon frequency and ϕ_0 is an initial phase difference. In Figs. 3(b)–3(d), we plot $S(k, \tilde{\tau})$ in the rescaled time $\tilde{\tau} = \gamma_{k,f}\tau$ and confirm that all spectra oscillate synchronously with a time period $\approx\pi$, thus validating the phonon interference picture. For comparison, we also plot the evolution of samples with a direct interaction quench from g_i to g_f without an MI period ($\Delta\tau = 0$). Oscillations in $S(k, \tilde{\tau})$ can also be observed, albeit with smaller amplitudes and phase offsets $\phi_0 \approx 0$, as these oscillations result solely from the interference of in phase quasiparticle projections from suddenly decreasing the Bogoliubov energy [13]. In either case, with or without MI, we observe that phase

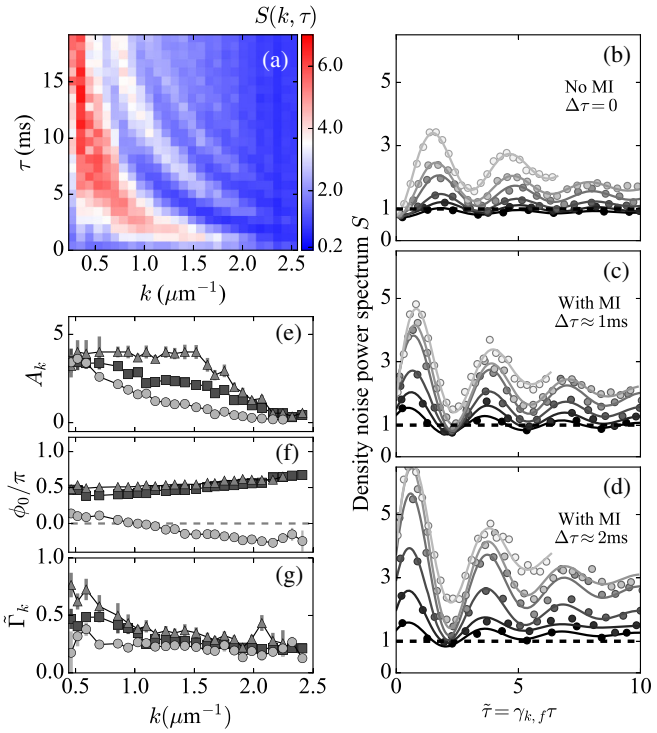

FIG. 3. Coherent oscillations in the density noise power spectrum. (a) Full evolution of the power spectrum $S(k,\tau)$ with $\Delta\tau \approx 1$ ms, showing coherent oscillations in time and k space. (b)–(d) Synchronized oscillations of $S(k,\tilde{\tau})$ plotted in the rescaled time unit $\tilde{\tau} = \gamma_{k,f}\tau$ for various $k \approx (1, 1.3, 1.6, 1.8, 2.1, 2.2)/\mu$m (gray circles from bright to dark). Horizontal dashed lines mark the atomic shot-noise limit. Solid lines are sinusoidal fits. Fitted amplitude A_k, phase offset ϕ_0, and decay rate $\tilde{\Gamma}_k$ from samples with $\Delta\tau \approx 0$ ms (filled circles), 1 ms (filled squares), and 2 ms (filled triangles) are plotted in (e)–(g), respectively.

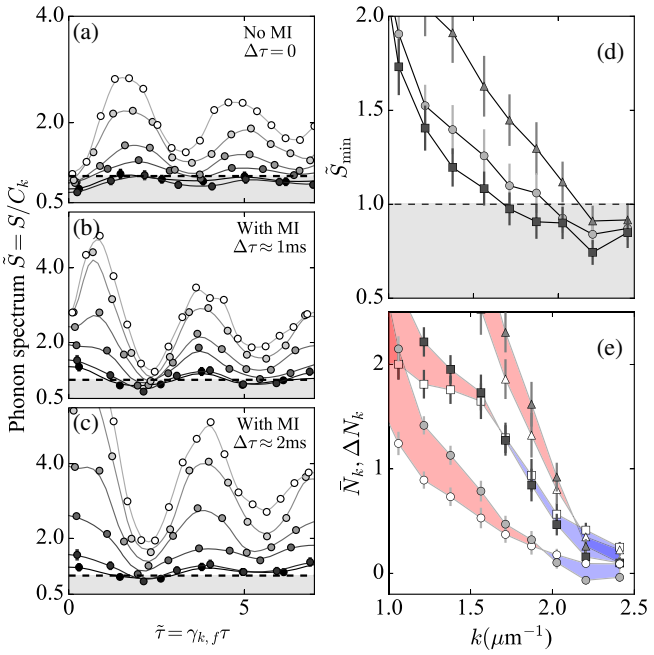

FIG. 4. Testing two-mode squeezing and quantum entanglement in the phonon basis. (a)–(c) Rescaled phonon spectrum $\tilde{S}(k,\tilde{\tau})$ for $k \approx (1.3, 1.6, 1.8, 2.1, 2.2, 2.4)/\mu$m (filled circles from bright to dark), evaluated using data as shown in Figs. 3(b)–3(d). Solid curves are guides to the eye. (d) First minima $\tilde{S}_{\min}$ in the phonon spectra of various wave numbers k, at $\Delta\tau \approx 0$ ms (filled circles), 1 ms (squares), and 2 ms (triangles), respectively. In (a)–(d), horizontal dashed lines mark the quantum limit, below which Eq. (1) is violated. Error bars include systematic and statistical errors. (e) Mean phonon population $\bar{N}_k$ (filled symbols) and pair-correlation amplitude ΔN_k (open symbols) extracted using the first minima and maxima identified in (a), circles; (b), squares; and (c), triangles, respectively. Blue (red) shaded areas mark the region where $\Delta N_k > \bar{N}_k$ ($\Delta N_k < \bar{N}_k$). Error bars represent statistical errors.

coherence is lost in a few cycles and the density noise spectra reach new steady-state values.

To quantify phase coherence and dissipation at final $g = g_f$, we perform simple sinusoidal fits $S(k,\tilde{\tau}) = S_f - S_o e^{-\tilde{\Gamma}_k\tilde{\tau}} - A_k e^{-\tilde{\Gamma}_k\tilde{\tau}}\cos(2\tilde{\tau} + \phi_0)$ to the data to extract (A_k, ϕ_0, $\tilde{\Gamma}_k$), as shown in Figs. 3(e)–3(g) (the steady-state values S_f and S_o are not shown). The larger oscillation amplitudes A_k found in samples with $\Delta\tau \approx 1$ ms and 2 ms show that MI-induced quasiparticles are highly phase coherent. This can also be seen in the nonzero phase offset $\phi_0 \gtrsim \pi/2$ at $k \gtrsim 0.5/\mu$m in Fig. 3(f), which is coherently accumulated during the MI period. Furthermore, in Fig. 3(g), we observe a nearly constant decay rate $\tilde{\Gamma}_k \approx 0.31(8)$ at $k \gtrsim 0.8/\mu$m for these MI-induced oscillations. This is close to the decay rate $\tilde{\Gamma}_k \approx 0.22(4)$ in samples without an MI period ($\Delta\tau = 0$), suggesting that the short MI dynamics does not heat up the sample significantly to increase the phonon dissipation rate.

We now focus on identifying a key signature of nonclassical correlations. To search for entanglement in the final phonon basis, we evaluate the squeezing parameter $C_k = \epsilon_k/\epsilon(k, g_f)$ at $g = g_f$ and plot the rescaled phonon spectra $\tilde{S}(k,\tilde{\tau}) = S(k,\tilde{\tau})/C_k$, as shown in Figs. 4(a)–4(c) [35]. In this basis, the phonon spectra at momenta $k \gtrsim 1.5/\mu$m can be observed to oscillate above and below the rescaled quantum limit $\tilde{S} = 1$, showing signatures of two-mode squeezing and antisqueezing as time evolves. The first minimum $\tilde{S}_{\min}$ identified at various momenta k is plotted in Fig. 4(d), in which we find that $\tilde{S}_{\min}$ violates the inequality Eq. (1) in a wider range for the MI sample with $\Delta\tau \approx 1$ ms than it does for the samples without MI or with longer $\Delta\tau$. The strongest violation is in the range of $2.1/\mu\text{m} \lesssim k \lesssim 2.2/\mu$m and has an average $\tilde{S}_{\min} \approx 0.77(7) < 1$, compared with $\tilde{S}_{\min} \approx 0.84(8)$ without MI and $\tilde{S}_{\min} \approx 0.91(5)$ for $\Delta\tau \approx 2$ ms. Lastly, we comment that the initial violation of inequality for samples without MI at $\tilde{\tau} \approx 0$ is also clear. However, fewer modes show squeezing when the phonon spectra return back to the first minima $\tilde{S}_{\min}$.

To further interpret our result, we extract the mean phonon number $\bar{N}_k$ and the pair-correlation amplitude ΔN_k by using the first maximum $\tilde{S}_{\max}$ and minimum $\tilde{S}_{\min}$ identified in $\tilde{S}(k,\tilde{\tau})$ at each k in Figs. 4(a)–4(c):

$$\bar{N}_k \approx \frac{\tilde{S}_{\max}+\tilde{S}_{\min}}{2}-1$$
$$\Delta N_k \approx \frac{\tilde{S}_{\max}-\tilde{S}_{\min}}{2}. \quad (3)$$

As shown in Fig. 4(e), both $\bar{N}_k$ and ΔN_k have comparably increased due to pair production in MI samples of $\Delta\tau \neq 0$. Quantum entanglement appears to better prevail for $\Delta\tau \approx 1$ ms and at $k \gtrsim 1.5/\mu$m, where $\Delta N_k \gtrsim \bar{N}_k$. This may be understood as any excessive incoherent population $\bar{N}_k - \Delta N_k > 0$ in our samples can be due partially to quasiparticle dissipation during the quench and partially to incoherent (thermal) phonons present in the initial state. The latter are better suppressed at $k > 1.5/\mu$m as $\epsilon(k,g_i) > k_B T \approx \hbar \times 1$ kHz.

In summary, we observe pair-correlation signal and nonclassical correlation in atomic quantum gases quenched to an attractive interaction, with two-mode squeezing $\tilde{S}_{\min} \approx 0.8 < 1$ below the quantum limit. Further reduction of initial incoherent phonon populations or of decoherence during pair-production processes may increase the nonclassical signal in future experiments. Reaching $\tilde{S} < 0.5$ could open up applications requiring Einstein–Podolsky–Rosen entangled quasiparticle pairs [36–40]. Our method may be extended to analyze entanglement distribution between noncausal regions before the interaction quench. Furthermore, analogously to the discussion in Ref. [41], extending our analyses of two-mode quadrature variance to skewness [42] and other higher-order correlation terms may provide necessary observables for probing entanglement entropy and transport in a quantum gas.

We thank M. Kruczenski and Q. Zhou for discussions. This work is supported in part by the DOE QuantISED program (through Grant No. DE-SC0019202 and the consortium "Intersections of QIS and Theoretical Particle Physics" at Fermilab) and the W. M. Keck Foundation. C.-A. C. and C.-L. H. acknowledge support by the NSF (Grant No. PHY-1848316).

*clhung@purdue.edu

[1] T. E. Keller and M. H. Rubin, Theory of two-photon entanglement for spontaneous parametric down-conversion driven by a narrow pump pulse, Phys. Rev. A **56**, 1534 (1997).

[2] J.-W. Pan, Z.-B. Chen, C.-Y. Lu, H. Weinfurter, A. Zeilinger, and M. Żukowski, Multiphoton entanglement and interferometry, Rev. Mod. Phys. **84**, 777 (2012).

[3] J. Eisert, M. Friesdorf, and C. Gogolin, Quantum many-body systems out of equilibrium, Nat. Phys. **11**, 124 (2015).

[4] S. Finazzi and I. Carusotto, Entangled phonons in atomic bose-einstein condensates, Phys. Rev. A **90**, 033607 (2014).

[5] P. Jurcevic, B. P. Lanyon, P. Hauke, C. Hempel, P. Zoller, R. Blatt, and C. F. Roos, Quasiparticle engineering and entanglement propagation in a quantum many-body system, Nature (London) **511**, 202 (2014).

[6] M. Cheneau, P. Barmettler, D. Poletti, M. Endres, P. Schauß, T. Fukuhara, C. Gross, I. Bloch, C. Kollath, and S. Kuhr, Light-cone-like spreading of correlations in a quantum many-body system, Nature (London) **481**, 484 (2012).

[7] P. Calabrese and J. Cardy, Entanglement entropy and quantum field theory, J. Stat. Mech. (2004) P06002.

[8] D. A. Abanin, E. Altman, I. Bloch, and M. Serbyn, Colloquium: Many-body localization, thermalization, and entanglement, Rev. Mod. Phys. **91**, 021001 (2019).

[9] J. Steinhauer, Observation of quantum hawking radiation and its entanglement in an analogue black hole, Nat. Phys. **12**, 959 (2016).

[10] J. R. M. de Nova, K. Golubkov, V. I. Kolobov, and J. Steinhauer, Observation of thermal hawking radiation and its temperature in an analogue black hole, Nature (London) **569**, 688 (2019).

[11] J. Hu, L. Feng, Z. Zhang, and C. Chin, Quantum simulation of unruh radiation, Nat. Phys. **15**, 785 (2019).

[12] J.-C. Jaskula, G. B. Partridge, M. Bonneau, R. Lopes, J. Ruaudel, D. Boiron, and C. I. Westbrook, Acoustic Analog to the Dynamical Casimir Effect in a Bose-Einstein Condensate, Phys. Rev. Lett. **109**, 220401 (2012).

[13] C.-L. Hung, V. Gurarie, and C. Chin, From cosmology to cold atoms: observation of sakharov oscillations in a quenched atomic superfluid, Science **341**, 1213 (2013).

[14] M. Schemmer, A. Johnson, and I. Bouchoule, Monitoring squeezed collective modes of a one-dimensional bose gas after an interaction quench using density-ripple analysis, Phys. Rev. A **98**, 043604 (2018).

[15] A. Rançon, C.-L. Hung, C. Chin, and K. Levin, Quench dynamics in bose-einstein condensates in the presence of a bath: Theory and experiment, Phys. Rev. A **88**, 031601(R) (2013).

[16] K. E. Strecker, G. B. Partridge, A. G. Truscott, and R. G. Hulet, Formation and propagation of matter-wave soliton trains, Nature (London) **417**, 150 (2002).

[17] J. H. Nguyen, D. Luo, and R. G. Hulet, Formation of matter-wave soliton trains by modulational instability, Science **356**, 422 (2017).

[18] P. Everitt, M. Sooriyabandara, M. Guasoni, P. Wigley, C. Wei, G. McDonald, K. Hardman, P. Manju, J. Close, C. Kuhn *et al.*, Observation of a modulational instability in bose-einstein condensates, Phys. Rev. A **96**, 041601(R) (2017).

[19] T. Mežnaršič, T. Arh, J. Brence, J. Pišljar, K. Gosar, Ž. Gosar, R. Žitko, E. Zupanič, and P. Jeglič, Cesium bright matter-wave solitons and soliton trains, Phys. Rev. A **99**, 033625 (2019).

[20] J. Sanz, A. Frölian, C. Chisholm, C. Cabrera, and L. Tarruell, Interaction control and bright solitons in coherently-coupled bose-Einstein condensates, arXiv:1912.06041.

[21] C.-A. Chen and C.-L. Hung, Observation of Universal Quench Dynamics and Townes Soliton Formation from

Modulational Instability in Two-Dimensional Bose Gases, Phys. Rev. Lett. **125**, 250401 (2020).
[22] Z. Tian, S.-Y. Chä, and U. R. Fischer, Roton entanglement in quenched dipolar bose-einstein condensates, Phys. Rev. A **97**, 063611 (2018).
[23] J. Steinhauer, Measuring the entanglement of analogue hawking radiation by the density-density correlation function, Phys. Rev. D **92**, 024043 (2015).
[24] A. Furusawa, J. L. Sørensen, S. L. Braunstein, C. A. Fuchs, H. J. Kimble, and E. S. Polzik, Unconditional quantum teleportation, Science **282**, 706 (1998).
[25] S. L. Braunstein and H. J. Kimble, Teleportation of Continuous Quantum Variables, Phys. Rev. Lett. **80**, 869 (1998).
[26] A. I. Lvovsky and M. G. Raymer, Continuous-variable optical quantum-state tomography, Rev. Mod. Phys. **81**, 299 (2009).
[27] A. J. Ferris, M. K. Olsen, E. G. Cavalcanti, and M. J. Davis, Detection of continuous variable entanglement without coherent local oscillators, Phys. Rev. A **78**, 060104(R) (2008).
[28] See Supplemental Material at http://link.aps.org/supplemental/10.1103/PhysRevLett.127.060404 for experimental calibration, theory calculations, and fits.
[29] L.-M. Duan, G. Giedke, J. I. Cirac, and P. Zoller, Inseparability Criterion for Continuous Variable Systems, Phys. Rev. Lett. **84**, 2722 (2000).
[30] R. Simon, Peres-Horodecki Separability Criterion for Continuous Variable Systems, Phys. Rev. Lett. **84**, 2726 (2000).
[31] S. Robertson, F. Michel, and R. Parentani, Controlling and observing nonseparability of phonons created in time-dependent 1d atomic bose condensates, Phys. Rev. D **95**, 065020 (2017).
[32] S. Robertson, F. Michel, and R. Parentani, Assessing degrees of entanglement of phonon states in atomic bose gases through the measurement of commuting observables, Phys. Rev. D **96**, 045012 (2017).
[33] C. Chin, R. Grimm, P. Julienne, and E. Tiesinga, Feshbach resonances in ultracold gases, Rev. Mod. Phys. **82**, 1225 (2010).
[34] C.-L. Hung, X. Zhang, L.-C. Ha, S.-K. Tung, N. Gemelke, and C. Chin, Extracting density–density correlations from in situ images of atomic quantum gases, New J. Phys. **13**, 075019 (2011).
[35] We note a $\pm 20\%$ variation of mean density across the analysis region ($38 \times 38\ \mu\mathrm{m}^2$). As a result, the squeezing parameter C_k has at most a small $\pm 4\%$ variation relative to the mean within the reported momentum range as shown in Fig. 4.
[36] M. D. Reid and P. D. Drummond, Quantum Correlations of Phase in Nondegenerate Parametric Oscillation, Phys. Rev. Lett. **60**, 2731 (1988).
[37] J. Peise, I. Kruse, K. Lange, B. Lücke, L. Pezzè, J. Arlt, W. Ertmer, K. Hammerer, L. Santos, A. Smerzi *et al.*, Satisfying the einstein–podolsky–rosen criterion with massive particles, Nat. Commun. **6**, 1 (2015).
[38] M. Fadel, T. Zibold, B. Décamps, and P. Treutlein, Spatial entanglement patterns and einstein-podolsky-rosen steering in bose-einstein condensates, Science **360**, 409 (2018).
[39] P. Kunkel, M. Prüfer, H. Strobel, D. Linnemann, A. Frölian, T. Gasenzer, M. Gärttner, and M. K. Oberthaler, Spatially distributed multipartite entanglement enables epr steering of atomic clouds, Science **360**, 413 (2018).
[40] K. Lange, J. Peise, B. Lücke, I. Kruse, G. Vitagliano, I. Apellaniz, M. Kleinmann, G. Tóth, and C. Klempt, Entanglement between two spatially separated atomic modes, Science **360**, 416 (2018).
[41] I. Klich and L. Levitov, Quantum Noise as an Entanglement Meter, Phys. Rev. Lett. **102**, 100502 (2009).
[42] J. Armijo, T. Jacqmin, K. V. Kheruntsyan, and I. Bouchoule, Probing Three-Body Correlations in a Quantum Gas Using the Measurement of the Third Moment of Density Fluctuations, Phys. Rev. Lett. **105**, 230402 (2010).